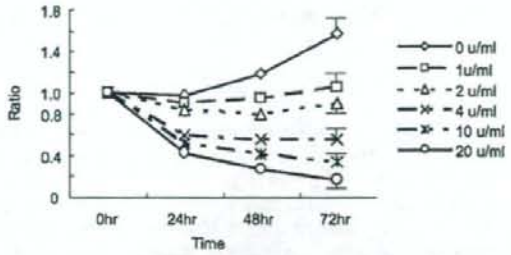

Fig. 4. Dose-dependent inhibition of replication by interferon-α (IFN). OR6 cells were transfected with wild-type replicon (OR/3-5B/KE). Inhibition of HCV RNA replication in the OR6c cell treated with IFN-α was shown at the indicated time (24, 48, and 72 hr) from the start of treatment. The cells were treated with IFN-α (0, 1, 2, 4, 10, and 20 u/ml), and the Renilla luciferase assay was performed as described in Materials and Methods Section. The relative luciferase activity (%) calculated at each point, where the luciferase activity of non-treated cells at 0 hr was assigned to be 100%, is presented. The data indicate means ± SD of triplicates from three independent experiments.

changed by these treatments (Fig. 6), indicating that both IFN and RBV were not toxic to the cells at the indicated concentrations. As shown in Figures 4 and 5, the inhibition of HCV RNA replication occurred in a dose-dependent manner with IFN or RBV treatments. RBV at a concentration of 100 μM inhibited replication of RNA (Fig. 5), but was not toxic to OR6c cells (Fig. 6).

The inhibitory effect of 100 μM RBV on RNA replication in each mutant was also examined. Various biological effect of IFN has been investigated and its effect on cell cycle or cell-differentiation is strong, and we focused on the effect of mutants on RBV treatment. To see this effect, we compared between IFN alone and IFN + RBV. As shown in Figure 7, no difference between three mutants was seen in the treatment with 1 unit/ml of IFN. The proliferation of each mutant RNA was similarly reduced to around a ratio of 0.6. On the other hand, addition of 100 μM of RBV was differently affected by each mutation pattern (Fig. 8). The single mutant with V85I and double mutants with V85I and K124E

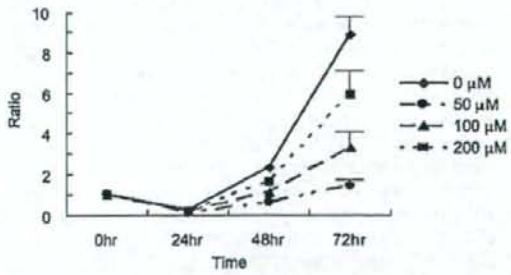

Fig. 5. Dose-dependent inhibition of HCV RNA replication by ribavirin. OR6 cells were transfected with wild-type replicon (OR/3-5B/KE) and treated with ribavirin at concentrations of 50, 100, and 200 μM for 72 hr. Inhibition of HCV RNA replication in the OR6c cell treated with ribavirin (RBV) was shown at the indicated time (24, 48, and 72 hr) from the start of treatment. The relative luciferase activity (%) calculated at each point, where the luciferase activity of non-treated cells at 0 hr was assigned to be 100%, is presented. The data indicate means ± SD of triplicates from three independent experiments.

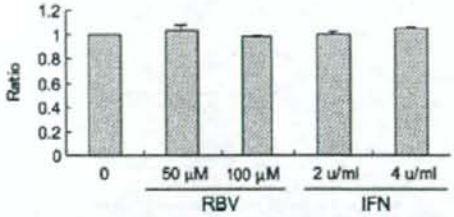

Fig. 6. Cytotoxicity of ribavirin (RBV) or interferon-α (IFN) on replicon RNA in OR6c cells. OR6c cells with OR/3-5B/KE RNA were cultured in the absence or presence of RBV or IFN (50 and 100 μM or 2 and 4 u/ml) for 72 hr, and then the cell viability was determined as described in Materials and Methods Section. The relative cell viability (%) calculated at each point, when viability of non-treated cells was assigned to be 100%, is presented. The data indicate means ± SD of triplicates from three independent experiments.

were significantly increased in RNA proliferation. The degree of inhibition by RBV in OR/3-5B/KE(V85I) and OR/3-5B/KE(V85I&K124E) was significantly lower than that in OR/3-5B/KE, although the difference of OR/3-5B/KE(K124E) was not significant.

Indirect Immunofluorescence

To confirm the presence of replicating full-length RNAs in cells selected for G418 resistance following transfection with ON/C-5B/KE(V85I), one G418-resistant cell colony was selected at random and clonally cultured. We confirmed HCV protein expression by indirect immunofluorescence imaging and observed core protein in the replicon cells (OR6) (Fig. 9c), HCV core protein was demonstrated in the clonally isolated cell line selected after transfection with ON/C-5B/KE(V85I)

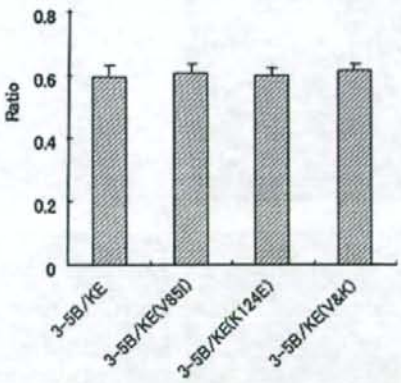

Fig. 7. Effect of interferon-α (IFN) on the subgenomic HCV replicon possessing the Renilla luciferase reporter. The replication levels of the subgenomic HCV replicons were monitored by luciferase reporter assay with IFN 0 u/ml or IFN 1 u/ml for 72 hr. Renilla luciferase assay was performed as described in Materials and Methods Section. The relative luciferase unit with IFN (1 u/ml) treatment were calculated, where the luciferase unit without IFN treatment was assigned to be 1, and compared between wild type (OR/3-5B/KE) and other three mutants (OR/3-5B/KE(V85I), OR/3-5B/KE(K124E), OR/3-5B/KE(V&K)). The data indicate means ± SD of triplicates from two independent experiments.

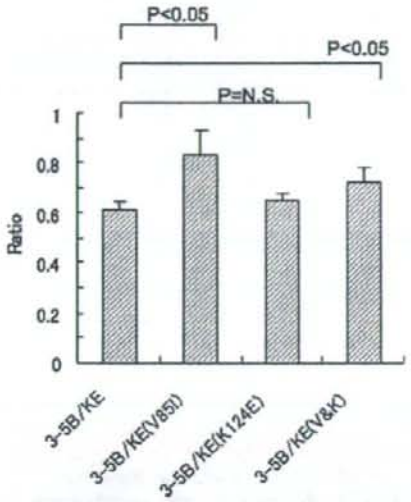

Fig. 8. Effect of interferon-α (IFN) and ribavirin (RBV) combination treatment on the replication levels of the subgenomic HCV replicon possessing the Renilla luciferase reporter. The replication levels of the subgenomic HCV replicons were monitored by luciferase reporter assay with IFN 1 u/ml or IFN 1 u/ml and ribavirin 100 μM for 72 hr. The relative luciferase unit of IFN 1 u/ml and ribavirin 100 mM treatment were calculated, where the luciferase unit of IFN 1 u/ml treatment was assigned to be 1, and compared in wild type (OR/3-5B/KE) and other three mutants (OR/3-5B/KE(V85I), OR/3-5B/KE(K124E), OR/3-5B/KE(V&K)). The data indicate means ± SD of triplicates from three independent experiments.

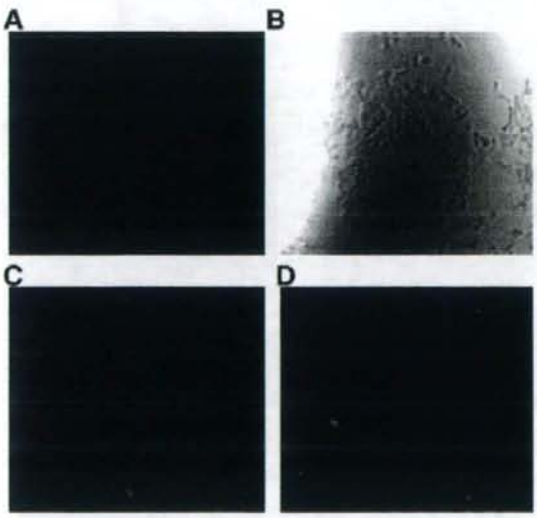

Fig. 9. Indirect immunofluorescence detection of HCV core antigen in normal OR6c cells (cured cell) (**a**), OR6 cells (wild-type HCV replicon) (**c**), and a clonally isolated cell line selected following transfection of OR6c cells with ON/3-5B/V85I (cell line 1) (**d**) and the correspondent phase-contrast microscopic photograph of OR6c cells (**b**).

(Fig. 9d), while it was not observed in the cured cell line (OR6C) (Fig. 9a,b).

DISCUSSION

Predictive factors for a sustained viral response (SVR) in IFN monotherapy or combination therapy have been vigorously investigated in prior studies. In addition to several host and viral factors, such as HCV genotypes, baseline viral load, stage of fibrosis, gender, age, and obesity [Saito et al., 2000, 2006], disappearance of serum HCV RNA during the early phase of therapy or a rapid decrease in HCV RNA levels are significant factors for achieving a SVR [Ferenci et al., 2001]. In our previous study, two distinct amino acid substitutions in the NS5B region of the HCV genome correlated with early viral responses in combination therapy [Kumagai et al., 2004]. NS5B of the HCV genome codes for RdRP, which regulates viral replication. Thus, the detected mutations might increase replication efficacy of HCV or induce resistance to the anti-viral effect of RBV, which could lead to resistance to therapy in the early phase. It was thought that the HCV replicon system would be a good tool for examining the correlation between viral mutation and replication capability. One of the mutation-introduced replicons (V85I) showed a higher replication activity than that of the wild type, and, consistent with our previous clinical study, this mutant was resistant to in vitro RBV treatment. The present study is the first to examine the precise relationship between such mutations and clinical data on the early clearance of HCV during IFN and RBV combination therapy. The mutations of V85I and K124E in NS5B have never been reported in the replicon system.

We investigated the effect of both IFN and RBV on the wild type and three mutants in NS5B at non-toxic concentration to the host cell (Fig. 6). One unit of IFN did not affect the replication of mutants (Fig. 7) but RBV significantly affected the replication of three mutants in the presence of IFN (Fig. 8). These results indicated that the polymorphism of NS5B affect sensitivity to RBV treatment. Although it has been known in the clinical setting that HCV RNA levels are not changed in patients with chronic hepatitis C during RBV monotherapy, our in vitro results showed the reduction of HCV RNA replication with RBV treatment. It was reported that serum levels of RBV in patients with chronic hepatitis C under IFN + RBV combination therapy was very low such as 10^{-14} mM [Naka et al., 2005], however, we can examine the anti-viral effect of much higher levels of RBV on the replicon system without a direct toxic effect of RBV in HuH7 cells. The possibility of a difference between circulating HCV particles and the replicon system in terms of RBV sensitivity may still exist, but this question will be further investigated using a recently developed cell culture system.

We used a dicistronic genome length and subgenome HCV RNA replication systems, which were established previously using HCV RNA from HCV-O infected in non-neoplastic human hepatocyte PH5CH8 cells. For the

cells into which genome-length and subgenomic HCV RNA were introduced, we chose the cloned cell line OR6c, prepared by IFN treatment from subgenomic HCV replicon-supporting cells, since OR6c had a higher efficiency of colony formation (ECF) than its parental HuH-7 cell line in a study of subgenomic HCV replicons [Blight et al., 2002]. It is known that the efficiency of colony formation is unstable, so that the luciferase activity and the colony-forming unit are always discrepant. The impact of ON/C-5B/KE(V85I) on colony formation was about 4 times that of the wild-type replicon in genome length and subgenomic RNAs, and the V85I mutation in NS5B showed 1.5 times higher replication activity in luciferase assay than the wild type in the subgenomic replicon system. Young et al. reported an RBV-resistant NS5B mutation during RBV monotherapy [Young et al., 2003], but this phenylalanine to tyrosine amino acid substitution located at the 415th position in NS5B differed from our amino acid substitution. Replicon cells were selected after G418 exposure, and the replication may be amplified by this selection culture. We sequenced the NS5B region, which includes the 85th and 124th nucleotide portions, from some clones 2 months after G418 selection culture, and we did not found significant mutations. From the present in vitro study and previous clinical study, it may be concluded that at least V85I mutation in NS5B increases viral replication that may cause resistance to RBV treatment.

Two of the patients in the clinical study [Kumagai et al., 2004] had previously been treated with IFN-α monotherapy in our previous study: one patient (Pt 3) has V85 and K124 in the HCV RdRP and the other (Pt 7) had I85 and E124. The former was a good responder to IFN-α and RBV combination therapy, but the latter was not. This result indicated that I85V and E124K substitutions did not affect the response to IFN-α monotherapy, because both types had failed to respond previously to IFN monotherapy. Therefore, we surmised that this amino acid substitution influenced the response to RBV anti-viral activity, which prompted us to examine the effect of RBV on viral replication. Several mechanisms of anti-viral activity of RBV have been proposed [Tam et al., 1999; Maag et al., 2001; Lau et al., 2002], but it is unclear why only the V85I single amino acid substitution induced replication better than the wild type. As shown previously [Kumagai et al., 2004], the 85th amino acid of HCV RdRP is distant from the active site of polymerase but is located near the RNA primer binding site, and this substitution may influence nucleotide misincorporation during polymerization. This 85th position is more important than the 124th position for replication of HCV-O.

This study is the first to examine whether NS5B polymorphism affects the replication efficiency and anti-HCV effect of RBV in an HCV RNA replicon system. It will be interesting to know whether these mutations in other genotypes (genotypes 2 and 3) replicate more efficiently and are more resistant than genotype 1b to RBV alone. Our data suggested that during clinical use of RBV, several mutations in the HCV genome might occur, such as in the isoleucine residue at the 85th position of HCV NS5B, which then affect viral replication and RBV resistance. This viral mutation may be one of the reasons for the failure in early viral clearance by IFN and RBV. There are, however, many factors that influence the success of IFN and RBV combination therapy. The resistance or sensitivity to IFN or peg-IFN, not to RBV, might also affect the early viral response, and many factors in both viral and host sides are known to affect IFN responsiveness, such as NS5A mutations [Enomoto et al., 1996], immunological status [Saito et al., 2000], or irf-1 gene promoter polymorphisms [Saito et al., 2002, 2005]. Together, these factors might determine the efficacy of anti-viral therapy in vivo, and the present in vitro data provides evidence partially supporting our clinical observations that NS5B polymorphisms are associated with early viral clearance during IFN and RBV therapy. However, it is unclear whether this single mutation occurs with peg-IFN plus RBV combination therapy and further studies are necessary. Nevertheless, our report is useful for modeling targets for antiviral compounds for the treatment of HCV.

REFERENCES

Blight KJ, McKeating JA, Rice CM. 2002. Highly permissive cell lines for subgenomic and genomic hepatitis C virus RNA replication. J Virol 76:13001–13014.

Bouvier-Alias M, Patel K, Dahari H, Beaucourt S, Larderie P, Blatt L, Hezode C, Picchio G, Dhumeaux D, Neumann AU, McHutchison JG, Pawlotsky JM. 2002. Clinical utility of total HCV core antigen quantification: A new indirect marker of HCV replication. Hepatology 36:211–218.

Contreras AM, Hiasa Y, He W, Terella A, Schmidt EV, Chung RT. 2002. Viral RNA mutations are region specific and increased by ribavirin in a full-length hepatitis C virus replication system. J Virol 76: 8505–8517.

Crotty S, Maag D, Arnold JJ, Zhong W, Lau JY, Hong Z, Andino R, Cameron CE. 2000. The broad-spectrum antiviral ribonucleoside ribavirin is an RNA virus mutagen. Nat Med 6:1375–1379.

Enomoto N, Sakuma I, Asahina Y, Kurosaki M, Murakami T, Yamamoto C, Ogura Y, Izumi N, Marumo F, Sato C. 1996. Mutations in the nonstructural protein 5A gene and response to interferon in patients with chronic hepatitis C virus 1b infection. N Engl J Med 334:77–81.

Feld JJ, Hoofnagle JH. 2005. Mechanism of action of interferon and ribavirin in treatment of hepatitis C. Nature 436:967–972.

Ferenci P, Brunner H, Nachbaur K, Datz C, Gschwantler M, Hofer H, Stauber R, Hackl F, Jessner W, Rosenbeiger M, Munda-Steindl P, Hegenbarth K, Gangl A, Vogel W. 2001. Combination of interferon induction therapy and ribavirin in chronic hepatitis C. Hepatology 34:1006–1011.

Fried MW, Shiffman ML, Reddy KR, Smith C, Marinos G, Goncales FL, Jr., Haussinger D, Diago M, Carosi G, Dhumeaux D, Craxi A, Lin A, Hoffman J, Yu J. 2002. Peginterferon alfa-2a plus ribavirin for chronic hepatitis C virus infection. N Engl J Med 347:975–982.

Gao B, Hong F, Radaeva S. 2004. Host factors and failure of interferon-alpha treatment in hepatitis C virus. Hepatology 39:880–890.

Ikeda M, Abe K, Dansako H, Nakamura T, Naka K, Kato N. 2005. Efficient replication of a full-length hepatitis C virus genome, strain O, in cell culture, and development of a luciferase reporter system. Biochem Biophys Res Commun 329:1350–1359.

Kumagai N, Takahashi N, Kinoshita M, Tsunematsu S, Tsuchimoto K, Saito H, Ishii H. 2004. Polymorphisms of NS5B protein relates to early clearance of hepatitis C virus by interferon plus ribavirin: A pilot study. J Viral Hepat 11:225–235.

Lanford RE, Guerra B, Lee H, Averett DR, Pfeiffer B, Chavez D, Notvall L, Bigger C. 2003. Antiviral effect and virus-host

interactions in response to alpha interferon, gamma interferon, poly(i)-poly(c), tumor necrosis factor alpha, and ribavirin in hepatitis C virus subgenomic replicons. J Virol 77:1092–1104.

Lau JY, Tam RC, Liang TJ, Hong Z. 2002. Mechanism of action of ribavirin in the combination treatment of chronic HCV infection. Hepatology 35:1002–1009.

Liang TJ, Rehermann B, Seeff LB, Hoofnagle JH. 2000. Pathogenesis, natural history, treatment, and prevention of hepatitis C. Ann Intern Med 132:296–305.

Lohmann V, Korner F, Dobierzewska A, Bartenschlager R. 2001. Mutations in hepatitis C virus RNAs conferring cell culture adaptation. J Virol 75:1437–1449.

Lukasiewicz E, Hellstrand K, Westin J, Ferrari C, Neumann AU, Pawlotsky JM, Schalm SW, Zeuzem S, Veldt BJ, Hansen BE, Verhey-Hart E, Lagging M. 2007. Predicting treatment outcome following 24 weeks peginterferon alpha-2a/ribavirin therapy in patients infected with HCV genotype 1: Utility of HCV-RNA at day 0, day 22, day 29, and week 6. Hepatology 45:258–259.

Maag D, Castro C, Hong Z, Cameron CE. 2001. Hepatitis C virus RNA-dependent RNA polymerase (NS5B) as a mediator of the antiviral activity of ribavirin. J Biol Chem 276:46094–46098.

Manns MP, McHutchison JG, Gordon SC, Rustgi VK, Shiffman M, Reindollar R, Goodman ZD, Koury K, Ling M, Albrecht JK. 2001. Peginterferon alfa-2b plus ribavirin compared with interferon alfa-2b plus ribavirin for initial treatment of chronic hepatitis C: A randomised trial. Lancet 358:958–965.

Naka K, Ikeda M, Abe K, Dansako H, Kato N. 2005. Mizoribine inhibits hepatitis C virus RNA replication: Effect of combination with interferon-α. Biochem Biophys Res Commun 330:871–879.

Pol S, Nalpas B, Bourliere M, Couzigou P, Tran A, Abergel A, Zarski JP, Berthelot P, Brechot C. 2000. Combination of ribavirin and interferon-alfa surpasses high doses of interferon-alfa alone in patients with genotype-1b-related chronic hepatitis C. Hepatology 31:1338–1344.

Poynard T, McHutchison J, Goodman Z, Ling MH, Albrecht J. 2000. Is an "a la carte" combination interferon alfa-2b plus ribavirin regimen possible for the first line treatment in patients with chronic hepatitis C? The ALGOVIRC Project Group. Hepatology 31:211–218.

Saito H, Ebinuma H, Satoh I, Miyaguchi S, Tada S, Iwabuchi N, Kumagai N, Tsuchimoto K, Morizane T, Ishii H. 2000. Immunological and virological predictors of outcome during interferon-alpha therapy of chronic hepatitis C. J Viral Hepat 7:64–74.

Saito H, Tada S, Wakabayashi K, Nakamoto N, Takahashi M, Nakamura M, Ebinuma H, Ishii H. 2002. The detection of IRF-1 promoter polymorphisms and their possible contribution to T helper 1 response in chronic hepatitis C. J Interferon Cytokine Res 22: 693–700.

Saito H, Tada S, Nakamoto N, Kitamura K, Horikawa H, Kurita S, Ebinuma H, Ishii H, Takahashi M, Tanaka S, Hibi T. 2005. Contribution of Irf-1 promoter polymorphisms to the Th1-type cell response and interferon-beta monotherapy for chronic hepatitis C. Hepatol Res 32:25–32.

Saito H, Tada S, Ebinuma H, Ishii H, Kashiwazaki K, Takahashi M, Tsukada N, Nishida J, Tanaka S, Shiozaki H, Hibi T. 2006. Role of erythrocytes as a reservoir for ribavirin and relationship with adverse reactions in the early phase of interferon combination therapy for chronic hepatitis C virus infections. J Clin Microbiol 44: 3562–3568.

Saracco G, Ciancio A, Olivero A, Smedile A, Roffi L, Croce G, Colletta C, Cariti G, Andreoni M, Biglino A, Calleri G, Maggi G, Tappero GF, Orsi PG, Terreni N, Macor A, Di Napoli A, Rinaldi E, Ciccone G, Rizzetto M. 2001. A randomized 4-arm multicenter study of interferon alfa-2b plus ribavirin in the treatment of patients with chronic hepatitis C not responding to interferon alone. Hepatology 34:133–138.

Sidwell RW, Huffman JH, Khare GP, Allen LB, Witkowski JT, Robins RK. 1972. Broad-spectrum antiviral activity of Virazole: 1-beta-D-ribofuranosyl-1,2,4-triazole-3-carboxamide. Science 177:705–706.

Takahashi M, Saito H, Higashimoto M, Atsukawa K, Ishii H. 2005. Benefit of hepatitis C virus core antigen assay in prediction of therapeutic response to interferon and ribavirin combination therapy. J Clin Microbiol 43:186–191.

Tam RC, Pai B, Bard J, Lim C, Averett DR, Phan UT, Milovanovic T. 1999. Ribavirin polarizes human T cell responses towards a Type 1 cytokine profile. J Hepatol 30:376–382.

Young KC, Lindsay KL, Lee KJ, Liu WC, He JW, Milstein SL, Lai MM. 2003. Identification of a ribavirin-resistant NS5B mutation of hepatitis C virus during ribavirin monotherapy. Hepatology 38: 869–878.

Zeuzem S, Lee JH, Franke A, Ruster B, Prummer O, Herrmann G, Roth WK. 1998. Quantification of the initial decline of serum hepatitis C virus RNA and response to interferon alfa. Hepatology 27:1149–1156.

Liver International ISSN 1478-3223

BASIC STUDIES

Mitochondrial electron transport inhibition in full genomic hepatitis C virus replicon cells is restored by reducing viral replication

Mie Ando[1], Masaaki Korenaga[2], Keisuke Hino[1], Masanori Ikeda[3], Nobuyuki Kato[3], Sohji Nishina[2], Isao Hidaka[2] and Isao Sakaida[2]

1 Department of Basic Laboratory Sciences, Yamaguchi University Graduate School of Medicine, Yamaguchi, Japan
2 Department of Gastroenterology and Hepatology, Yamaguchi University Graduate School of Medicine, Yamaguchi, Japan
3 Department of Molecular Biology, Okayama University Graduate School of Medicine, Dentistry, and Pharmaceutical Sciences, Okayama, Japan

Keywords
fluvastatin – interferon – oxidative stress – reactive oxygen species

Correspondence
Keisuke Hino, MD, PhD, Department of Hepatology and Pancreatology, Kawasaki Medical University, 577 Matsushima Kurashiki, Okayama 701-0192, Japan
Tel: +81 86 4621111
Fax: +81 86 4641196
e-mail: khino@med.kawasaki-m.ac.jp

Received 25 September 2007
Accepted 30 January 2008

DOI:10.1111/j.1478-3231.2008.01720.x

Abstract

Background/Aim: Hepatitis C virus (HCV) core protein has been shown to inhibit mitochondrial electron transport and to increase reactive oxygen species (ROS) *in vitro* and *in vivo*. The aim of this study was to investigate whether inhibiting HCV replication could restore the mitochondrial redox state and electron transport activity. *Methods:* We measured ROS, mitochondrial reduced glutathione content, and mitochondrial complex I, II, III and IV activities and protein expression in full genomic HCV replicon cells and cured cells that had been prepared by eliminating HCV RNA from replicon cells by interferon (IFN)-α treatment. *Results:* Cured cells had significantly lower ROS production and greater mitochondrial glutathione content than replicon cells. Complete inhibition of HCV replication by IFN-α restored complex I and IV activities by 20–30% ($P < 0.01$) and complex I expression ($P < 0.05$). Treatment with fluvastatin, one of the 3-hydroxy-3-methylglutaryl co-enzyme A reductase inhibitors, which is known to have anti-HCV activity, partially inhibited core protein expression and restored complex I activity in full genomic HCV replicon cells to a lesser degree ($P < 0.05$). *Conclusions:* Our results show that the mitochondrial redox state and electron transport activity can be restored by reducing HCV replication.

Hepatitis C virus (HCV) causes acute and chronic hepatitis, cirrhosis and hepatocellular carcinoma (HCC) (1). Because current antiviral treatment can only eliminate the virus in about 50% of patients (2, 3), therapies to reduce disease progression in chronically infected individuals would be of great benefit. In this respect, it is still a matter of debate whether reduction of HCV replication, even if not eliminating HCV, is beneficial to the outcome of disease. Although the mechanisms of its pathogenesis are incompletely understood, there have been several lines of evidence suggesting that oxidative stress is present in chronic hepatitis C to a greater degree than in other inflammatory liver diseases and is closely related to disease progression (4, 5). We and others have shown that HCV core protein induces the production of reactive oxygen species (ROS) (6–8) and that mitochondrial electron transport inhibition by HCV is associated with ROS production (9). Therefore, whether reduction of HCV replication restores mitochondrial electron transport activity is of interest in exploring treatments to reduce disease progression in HCV-associated chronic liver disease.

Establishment of the HCV subgenomic replicon has made it possible to assess the antiviral activities of interferon (IFN) and other reagents *in vitro* (10). We also developed a genome-length HCV RNA replication reporter system (11) and found that different statins, which are 3-hydroxy-3-methylglutaryl co-enzyme A reductase inhibitors, have different anti-HCV profiles while using this reporter system (12). In the present study, we chose to use fluvastatin, which exhibited the strongest inhibition of HCV replication among the statins (12), to reduce HCV replication in full genomic HCV replicon cells without complete inhibition. The aim of this study was to examine whether mitochondrial electron transport activity was restored by reduction of HCV replication.

Materials and methods

Cell cultures

Full genomic HCV replicon cells were described in detail by Ikeda *et al.* (11). Cells were cultured in Dulbecco's modified Eagle's medium supplemented with 10% fetal calf serum, penicillin, streptomycin and G418 (300 μg/ml; Calbiochem, Darmstadt, Germany) and passaged twice a week at a 5:1 split ratio. Cured cells were established by eliminating genome-length HCV RNA from replicon cells by IFN-α treatment (500 IU/ml for 2 weeks; Sigma-Aldrich, St Louis, MO, USA) without G418, as described (11). In some experiments, full genomic HCV replicon cells were incubated in the presence of 10 μmol/L fluvastatin (Novartis Pharmaceutical, Tokyo, Japan) for 96 h.

Measurement of reactive oxygen species

The cellular ROS level was measured by oxidation of the cell-permeable, oxidation-sensitive fluorogenic precursor dihydrodichlorocarboxyfluorescein diacetate (DCFDA; Molecular Probes Inc., Eugene, OR, USA). Cells in six-well plates were treated with tertiary butyl hydroperoxide (t-BOOH) for 5 h or not, followed by a 30-min incubation with DCFDA (500 nmol/L final concentration) at 37 °C. Fluorescence was measured with a CytoFluorII fluorescence plate reader (PerSeptive Biosystems, Framingham, MA, USA) at an excitation wavelength of 486 nm and an emission wavelength of 530 nm as described (7).

Localization of ROS production on the subcellular level was observed with a Zeiss (Oberkochen, Germany) LSM5 Pascal inverted laser scanning confocal microscope. Cells were pre-incubated with 5 μmol of hydroxyphenyl florescein (HPF, Alexis Corporation, Lausen, Switzerland) (13) for 5 min at 37 °C. They were then imaged at 30-s intervals after treatment with 10 nmol/L t-BOOH. The green fluorescence of HPF (excitation, 488 nm; emission, 505–530 nm) was observed after excitation with an argon–krypton laser.

Isolation of mitochondria

Mitochondrial pellets were obtained as described previously with some modification (7, 9). Briefly, harvested cells were centrifuged at 500*g* for 5 min. The pellets were homogenized with 25 strokes using a Dounce homogenizer (Wheaton Science Products, Millville, NJ, USA) and a tight-fitting pestle with isolation buffer [70 mM sucrose, 1 mM KH_2PO_4, 5 mM HEPES, 220 mM mannitol, 5 mM sodium succinate and 0.1% bovine serum albumin (BSA), pH 7.4]. The homogenate was centrifuged at 1330*g* for 5 min at 4 °C. The supernatant fraction was retained, whereas the pellet was washed with isolation buffer and centrifuged again. The combined supernatant fractions were centrifuged at 1000*g* for 15 min at 4 °C to obtain a crude mitochondrial pellet. Purified mitochondria were prepared by sucrose gradient (1.5 M sucrose and 1 M sucrose) centrifugation as described (14) with some modification. An aliquot was removed for determination of the protein concentration with the Bio-Rad protein DC assay kit (Bio-Rad, Hercules, CA, USA), using BSA as the standard.

Measurement of reduced glutathione content

Crude mitochondrial samples (3–4 mg of mitochondrial protein) were sonicated using a Sonifier cell disruptor 200 (VWR Scientific, Danbury, CT, USA) for 15 s at power setting 3 in ice-cold 5% metaphosphoric acid and centrifuged at 3000*g* at 4 °C for 10 min. The concentration of reduced glutathione was measured by the thioester method using a GSH-400 kit (Oxis International Inc., Portland, OR, USA).

Immunoblotting

Crude mitochondrial pellets were suspended in lysis buffer (T-PER Tissue Extraction Reagent; Pierce, Rockford, IL, USA) and centrifuged at 10 000*g* for 15 min at 4 °C. The supernatant (20 μg of protein) was separated by sodium dodecyl sulphate-polyacrylamide gel electrophoresis on 16% gel. The proteins were electrophoretically blotted onto polyvinylidene difluoride membranes (Millipore, Bedford, MA, USA), blocked overnight at 4 °C with 5% skim milk and 0.1% Tween 20 in Tris-buffered saline, and subsequently incubated for 1 h at room temperature with an anti-hepatitis C core protein antibody (1:1000, Affinity Bio Reagents, Golden, CO, USA), anti-OxPhos complex I antibody (1:1000), anti-OxPhos complex II antibody (1:2000), anti-OxPhos complex III antibody (1:2500) or anti-OxPhos complex IV antibody (1:1000, Molecular Probes Inc). The membranes were washed, incubated with appropriate secondary antibodies and detected with ECL™ Western blot detection reagents (Amersham Biosciences, Piscataway, NJ, USA). The degree of protein expression was expressed as the normalized quotient, which was derived by dividing the intensity of the blot density of each protein by that of β-actin protein.

Measurement of complex I, II, III and IV activities

Submitochondrial particles were prepared from mitochondria by incubation for 3 min at 37 °C followed by sonication in a microcentrifuge tube immersed in ice water. Forty micrograms of submitochondrial

particles was pelleted at 15 000*g* for 10 min. Enzyme activity assays were performed at 25 °C by a previously established method (15). Complex I [nicotinamide adenine dinucleotide (NADH)-decylubiquinone oxidoreductase] activity was measured as the initial (5 min) rate of decrease of A_{340} using the acceptor 2,3-dimethoxy-5-methyl-6-*n*-decyl-1,4-benzoquinone (DB 80 μM) and 200 μM NADH as the donor in 10 mM Tris (pH 8.0) buffer containing 1 mg/ml BSA, 0.24 mM KCN and 0.4 μM antimycin A. Complex II (succinate decylubiquinone 2,6-dichlorophenolindophenol reductase) activity was measured at 600 nm using 80 μM DCPIP as the acceptor and 10 mM succinate as the donor in 10 mM KH_2PO_4 (pH 7.8), 1 mg/ml BSA, 2 mM EDTA, in the presence of 0.24 mM KCN, 4 μM rotenone, 0.2 mM ATP and 0.4 μM antimycin A. Complex III (ubiquinol cytochrome *c* reductase) activity was measured at 550 nm using 40 μM oxidized cytochrome *c* as the acceptor and 80 μM decylubiquinol as the donor in 10 mM KH_2PO_4 (pH 7.8), 1 mg/ml BSA, 2 mM EDTA, in the presence of 0.24 mM KCN, 4 μM rotenone and 0.2 mM ATP for 2 min. Complex IV (cytochrome *c* oxidase) activity was measured using a cytochrome *c* oxidase assay kit (Sigma-Aldrich), following the manufacturer's instructions.

Statistical analysis

Quantitative values are expressed as mean ± standard deviation. Two groups were compared by the Student *t*-test. A P value of < 0.05 was considered to be significant. Two groups among multiple groups were compared by the rank-based, Kruskal–Wallis analysis of variance test followed by Scheffe's test.

Results

Increased reactive oxygen species production and mitochondrial oxidant status in full genomic hepatitis C virus replicon cells

To assess the effect of HCV replication on ROS production, we used the ROS-sensitive fluorescent probe DCFDA. As compared with cured cells, HCV replication increased ROS 1.4-fold (Fig. 1A). Because HCV infection results in an inflammatory response and an increase in the basal oxidative stress, we next determined the effect of an exogenous oxidant, 500 nmol/L t-BOOH, on ROS production. This treatment had no effect on cured cells, but increased ROS production in full genomic HCV replicon cells to a level 2.5-fold greater than that of cured cells (Fig. 1A; $P < 0.01$). Cells were then imaged by confocal microscopy at 30-s intervals after exposure to HPF, which is more sensitive to ROS production than DCFDA. As shown in Figure 1B, treatment with t-BOOH significantly increased the oxidized fluorescent product as time passed in full genomic HCV replicon cells, but not in cured cells ($P < 0.0005$). Thus, a small volume of exogenous oxidant (10 nmol/L) that did not induce ROS production in cured cells significantly increased ROS production in full genomic HCV replicon cells.

We previously demonstrated, by confocal microscopy, that the mitochondria are the primary site of initial ROS production in cells expressing HCV core protein and cytochrome P450 2E1 (7). Because confocal microscopic images of the oxidized fluorescent product in replicon cells were almost the same as those in our previous study, we measured mitochondrial reduced glutathione content to assess mitochondrial antioxidant capacity. The level of mitochondrial reduced glutathione was significantly lower in full genomic HCV replicon cells than in cured cells (Fig. 1C; $P < 0.05$), suggesting that HCV replication was responsible for the mitochondrial oxidant status and sensitized to exogenous oxidative stress.

Restoration of mitochondrial electron transport activity by complete inhibition of hepatitis C virus replication

Our previous study has demonstrated that core protein causes oxidation of the glutathione pool, increases ROS production and inhibits complex I activity (9). Because increased ROS production and mitochondrial oxidant status were found in full genomic HCV replicon cells as well, we next measured complex I, II, III and IV activities in submitochondrial particles to determine whether inhibiting HCV replication restored mitochondrial electron transport activity. Complete inhibition of HCV replication by IFN-α restored complex I and IV activities by 20–30% ($P < 0.01$) (Fig. 2). However, complex II and III activities were not changed after treatment with IFN-α in these cells (Fig. 2).

We further assessed the expression levels of complexes I, II, III and IV in full genomic HCV replicon cells and cured cells. As shown in Figure 3, immunoblotting revealed that complete inhibition of HCV replication by IFN-α restored the complex I expression as well ($P < 0.05$). Although the complex IV activity was restored by IFN-α, the expression of complex IV did not change after complete inhibition of HCV replication. Thus, it should be noted that both activity and expression of complex I were restored by completely inhibiting HCV replication in full genomic HCV

Liver International (2008)

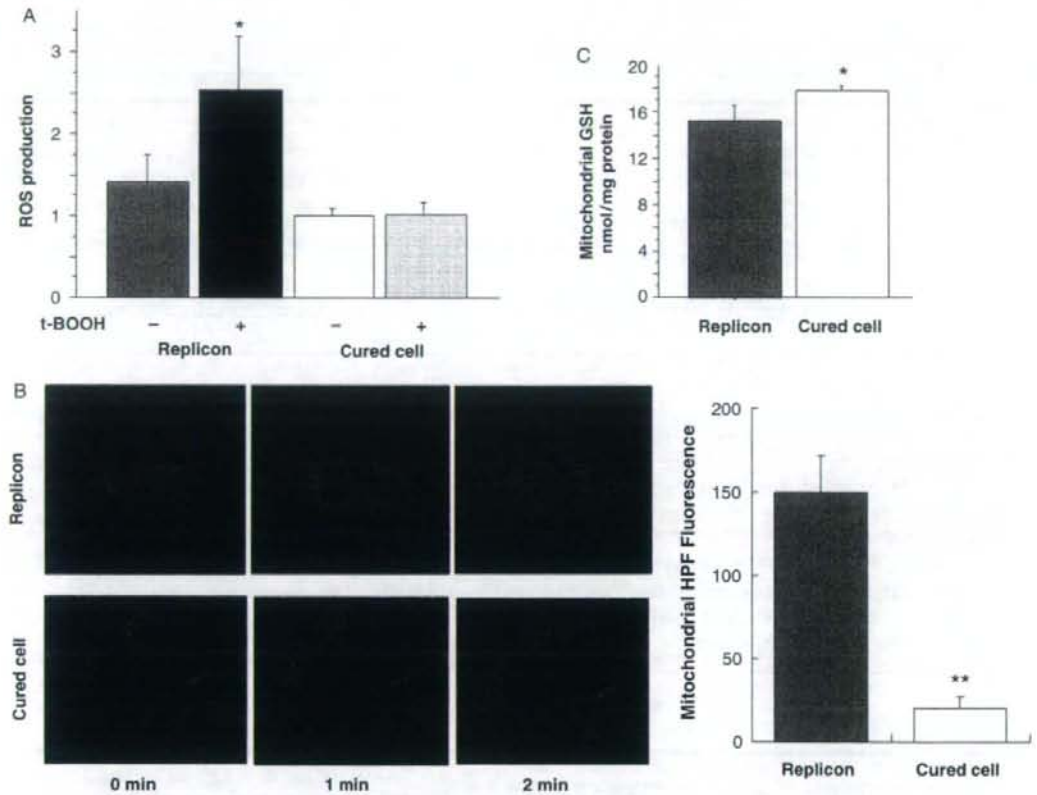

Fig. 1. Effects of HCV replication on ROS production and mitochondrial reduced glutathione level. (A) ROS production was measured by oxidation of DCFDA in HCV replicon cells and cured cells under control conditions or after 5-h incubation with t-BOOH (500 nmol/L). $^{*}P < 0.01$ compared with untreated cured cells. (B) Confocal images of ROS generation. HCV replicon cells and cured cells were pre-incubated with HPF, subsequently treated with t-BOOH (10 nmol/L) and imaged at 30-s intervals. The increase in HPF fluorescence intensity 2 min after treatment with t-BOOH was compared between HCV replicon cells and cured cells. $^{**}P < 0.0005$ compared with HCV replicon cells. (C) Reduced glutathione content was measured in crude mitochondrial fractions prepared from HCV replicon cells and cured cells. $^{*}P < 0.05$ compared with HCV replicon cells. DCFDA, dihydrodichlorocarboxyfluorescein diacetate; HCV, hepatitis C virus; HPF, hydroxyphenyl florescein; ROS, reactive oxygen species.

replicon cells, even though the significance of reduced complex IV activity remains elusive.

Incompletely inhibited hepatitis C virus replication partially restores mitochondrial electron transport activity

Fluvastatin, a 3-hydroxy-3-methylglutaryl co-enzyme A reductase inhibitor, has been shown to have an inhibitory effect on HCV replication in the present full genomic HCV replicon cells (12). We used fluvastatin for partially inhibiting HCV replication in full genomic HCV replicon cells, because it has a lesser inhibitory effect on HCV replication than IFN-α (12). In fact, expression of core protein was present in mitochondria, but was significantly lowered by treatment with fluvastatin in full genomic HCV replicon cells ($P < 0.05$; Fig. 4A). Partial inhibition of HCV replication restored complex I activity by ~13% ($P < 0.05$; Fig. 4B). Although statins including fluvastatin are known to have an anti-oxidative effect (16, 17), treatment with fluvastatin did not improve complex I activity in cured cells (Fig. 4B), suggesting that this activity was restored by its inhibitory effect on HCV replication rather than its anti-oxidative property. However, partial inhibition of HCV replication did

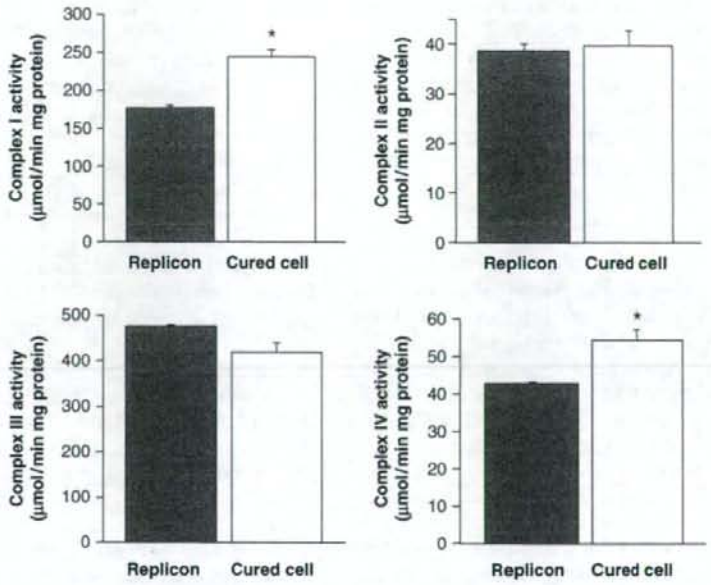

Fig. 2. Mitochondrial complex I, II, III and IV activities. Complex I (NADH-decylubiquinone oxidoreductase) activity, complex II (succinate decylubiquinone 2,6-dichlorophenolindophenol reductase) activity, complex III (ubiquinol cytochrome *c* reductase) activity and complex IV (cytochrome *c* oxidase) activity were measured in submitochondrial fractions prepared from HCV replicon cells and cured cells. $^*P < 0.01$ compared with HCV replicon cells. HCV, Hepatitis C virus; NADH, nicotinamide adenine dinucleotide.

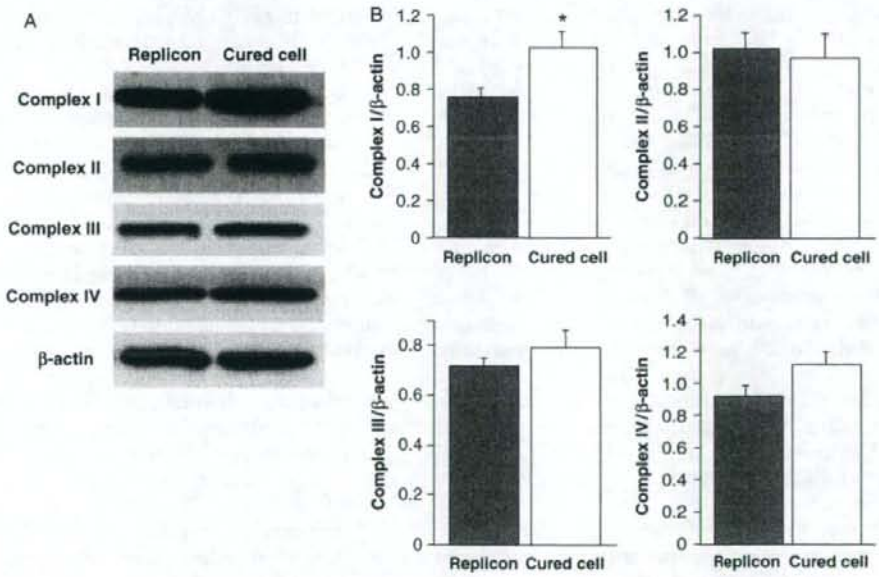

Fig. 3. Expression of mitochondrial complex I, II, III and IV. (A) Immunoblots for complex I, II, III and IV were performed using crude mitochondrial fractions prepared from HCV replicon cells and cured cells. (B) The degree of protein expression was normalized with β-actin protein. $^*P < 0.05$ compared with HCV replicon cells. HCV, hepatitis C virus.

Liver International (2008)

not lead to a significant reduction of ROS production (Fig. 4C), a significantly increased level of mitochondrial reduced glutathione (Fig. 4D) or complex I expression (Fig. 4A). Thus, incomplete inhibition of HCV replication restored mitochondrial electron transport activity in full genomic HCV replicon cells, even though it was not sufficient to reduce mitochondrial oxidative status.

Discussion

We have previously reported that HCV core protein inhibits mitochondrial electron transport and increases ROS production in the transgenic mouse liver (9). Our present results have shown that these phenomena can be reproduced in the presence of HCV replication. As replication of a full-length HCV genome rather than mere core protein expression is closer to the disease condition occurring in patients with chronic hepatitis C, the present results have strengthened the possibility that mitochondrial oxidation, ROS production and inhibition of mitochondrial electron transport are actually caused in chronic hepatitis C. Thanks to the establishment of HCV replicon cells, we could investigate the effect of inhibiting HCV replication on mitochondrial electron transport activity that was closely related to ROS production. In the present study, we focused on restoration of mitochondrial electron transport activity by inhibiting HCV replication, regarding complete inhibition of HCV replication *in vitro* as that of HCV eradicated with IFN therapy and partial inhibition of HCV replication *in vitro* as that in cells undergoing IFN therapy without HCV eradication.

Consistent with a previous observation, complex I activity, but not complex III activity, was reduced in full genomic HCV replicon cells. Complex I appeared to be the source of HCV-induced ROS, because mitochondrial ROS generation can occur at either complex I or complex III (18–20). We also found decreased expression of complex I in full genomic HCV replicon cells as compared with cured cells. Complex I is the site most sensitive to oxidative damage of the electron transport carriers, and inhibition of complex I occurs during the early stages of mitochondrial damage (21). Increased mitochondrial ROS production due to reduction of complex I activity amplifies mitochondrial oxidation, which in turn may inhibit the expression of complex I. Complex IV activity, i.e. that of cytochrome *c* oxidase, was reduced in full genomic HCV replicon cells as well. Complex IV localizes at the end of mitochondrial electron transport, accepts one electron at a time from cytochrome *c* and passes them four at a time to oxygen. Therefore, decreased activity of complex IV may amplify mitochondrial ROS production, possibly by inhibiting electron flow in the respiratory chain.

Thus, it is likely that HCV replication increases mitochondrial ROS production through inhibition of electron transport, causing oxidative stress within the liver in patients with chronic hepatitis C. Several different experimental models of HCV protein expression reproduced this finding (6–8). However, whether reduction of HCV replication restores mitochondrial function remains unknown. In the present study full genomic HCV replicon cells had ~30% reduction of complex I activity ($P = 0.0001$) and ~20% reduction in complex IV activity ($P < 0.01$) as compared with cured cells (Fig. 2). In other words, complete inhibition of HCV replication by IFN-α restored the activities of complex I and complex IV, leading to reduced ROS production in the presence of an exogenous oxidant and to an increase of mitochondrial reduced glutathione content (Fig. 1). There have been several lines of clinical evidence suggesting that HCV elimination by IFN treatment reverses the progression of liver fibrosis and significantly suppresses the development of HCC afterwards (22, 23). Restoration of mitochondrial electron transport activity by complete inhibition of HCV replication may well account for this clinical evidence, because the progression of liver fibrosis and development of HCC in chronic hepatitis C have been shown to be closely related to excess oxidative stress within the liver (24, 25).

In the clinical setting, however, HCV eradication by combination therapy with peginterferon-α and ribavirin has been successful in 50–60% of patients with refractory chronic hepatitis C at most (2, 3). Therefore, it is a critical issue for patients for whom this is unsuccessful if needed, whether prolonged reduction of HCV replication, not elimination of HCV, reduces or delays the progression of liver fibrosis and development of HCC. Although there have been several studies suggesting the inhibitory effect of IFN therapy on HCC development in patients with HCV-associated chronic liver diseases (26, 27), it is still controversial (28). Cured cells did not show core protein expression at all (data not shown), whereas fluvastatin-treated replicon cells had core protein expression that was significantly lower than in replicon cells without treatment. Thus, incomplete inhibition of HCV replication by fluvastatin was useful as a model for assessing if reduction of HCV replication, not elimination of HCV, could restore mitochondrial function. We found that incomplete inhibition of HCV replication restored complex I activity, but did

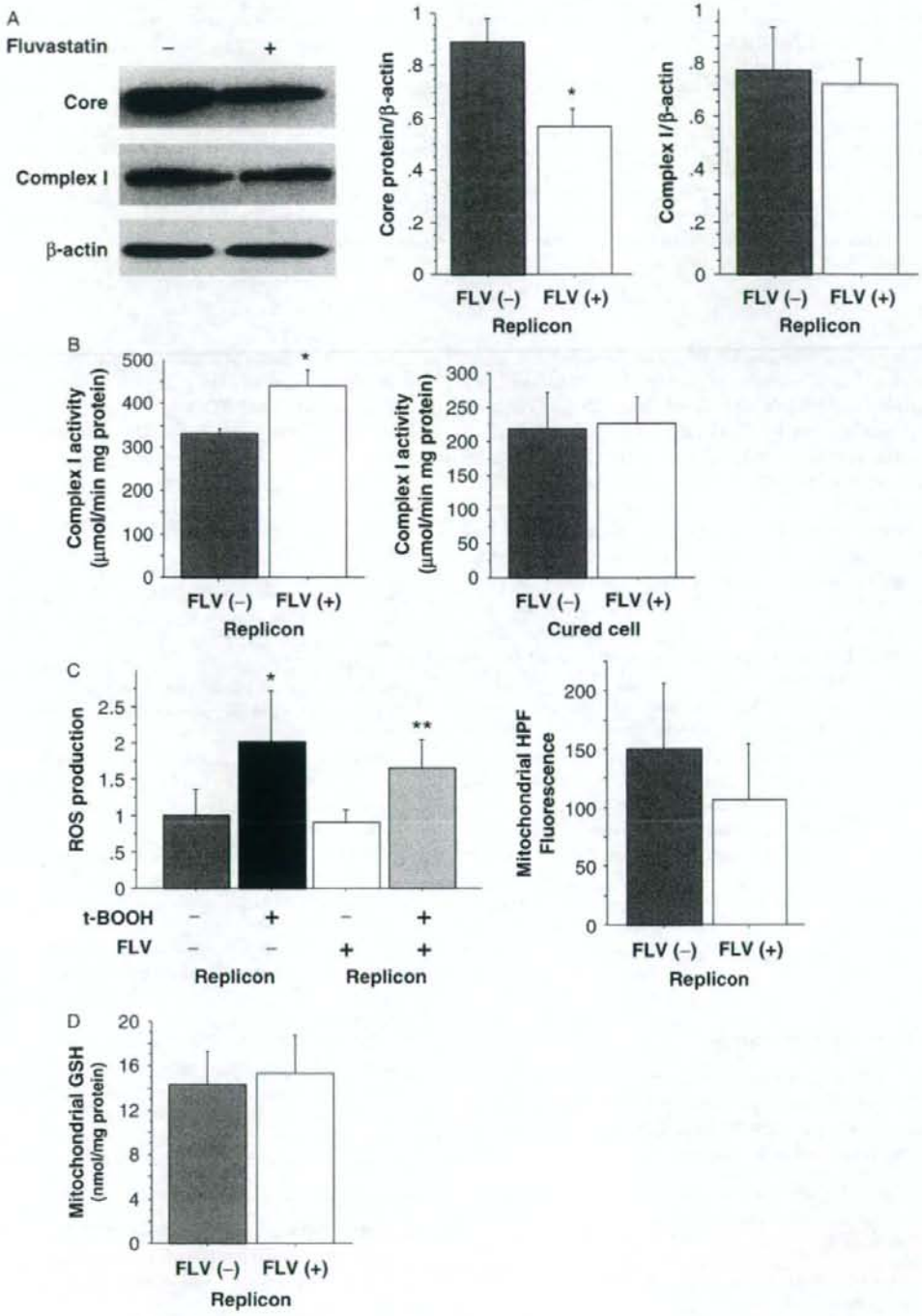

Liver International (2008)

Fig. 4. Effect of fluvastatin on core protein expression, mitochondrial complex I activity and expression, ROS production and mitochondrial reduced glutathione level. (A) Immunoblots for core protein and complex I were performed using crude mitochondrial fractions prepared from HCV replicon cells treated with/without fluvastatin. The degree of protein expression was normalized with β-actin protein. (B) Complex I (NADH-decylubiquinone oxidoreductase) activity was measured in submitochondrial fractions prepared from HCV replicon cells and cured cells, both of which were treated with/without fluvastatin. (C) ROS production was measured by oxidation of DCFDA in HCV replicon cells treated with/without fluvastatin under control conditions or after 5-h incubation with t-BOOH (500 nmol/L). HCV replicon cells treated with/without fluvastatin also were pre-incubated with HPF and subsequently treated with t-BOOH (10 nmol/L). The increase in HPF fluorescence intensity 2 min after treatment with t-BOOH was compared between HCV replicon cells with fluvastatin and those without. $^{*}P < 0.05$ as compared with HCV replicon cells without both t-BOOH and fluvastatin treatment. $^{**}P < 0.005$ as compared with fluvastatin-treated HCV replicon cells without t-BOOH. (D) Reduced glutathione content was measured in crude mitochondrial fractions prepared from HCV replicon cells treated with/without fluvastatin. DCFDA, dihydrodichlorocarboxyfluorescein diacetate; FLV, fluvastatin; HCV, hepatitis C virus; HPF, hydroxyphenyl florescein; NADH, nicotinamide adenine dinucleotide; ROS, reactive oxygen species; t-BOOH, tertiary butyl hydroperoxide.

not lead to the reduction of mitochondrial oxidative status. Thus it should be noted that restoration of complex I activity resulted from the inhibitory effect of HCV replication by fluvastatin rather than its antioxidant property. Even if incomplete inhibition of HCV replication fails to reduce mitochondrial oxidative status *in vitro*, restoration of complex I activity for a certain period *in vivo* may lead to a reduction of mitochondrial oxidative status. However, we need to recognize that inhibition of HCV replication *in vitro* by statins does not necessarily imply the same effect *in vivo*, because the absence of a clinical anti-HCV effect of statins has been reported (29). The present results showing that even incomplete inhibition of HCV replication can restore mitochondrial function to a lesser degree than completely inhibited HCV replication provides us with a rationale for suppressing HCV replication by anti-HCV agents in nonsustained responders to the current combination therapy.

In conclusion, our study shows that HCV replication causes oxidation of the mitochondrial glutathione pool, increases ROS production and inhibits mitochondrial electron transport activity, and that these changes in the mitochondrial redox state can be reversed by reducing HCV replication.

Acknowledgements

This study was supported by grants from the Ministry of Education, Culture, Sports, Science and Technology (No. 15590653 and No. 18590736), and in part by the Ministry of Health, Labor and Welfare, Japan.

References

1. Seeff LB. Natural history of chronic hepatitis C. *Hepatology* 2002; **36**: S35–46.
2. Fried MW, Shiffman ML, Reddy KR, *et al.* Peginterferon alfa-2a plus ribavirin for chronic hepatitis C virus infection. *N Engl J Med* 2002; **347**: 975–82.
3. Davis GL. Current therapy for chronic hepatitis C. *Gastroenterology* 2000; **118**: S104–14.
4. Barbaro G, Di Lorenzo G, Asti AM, *et al.* Hepatocellular mitochondrial alterations in patients with chronic hepatitis C: ultrastructural and biochemical findings. *Am J Gastroenterol* 1999; **942**: 198–205.
5. Valgimigli M, Valgimigli L, Trere D, *et al.* Oxidative stress EPR measurement in human liver by radical-probe technique. Correlation with etiology, histology and cell proliferation. *Free Radic Res* 2002; **36**: 939–48.
6. Okuda M, Li K, Beard MR, *et al.* Mitochondrial injury, oxidative stress, and antioxidant gene expression are induced by hepatitis C virus core protein. *Gastroenterology* 2002; **122**: 366–75.
7. Otani K, Korenaga M, Beard MR, *et al.* Hepatitis C virus core protein, cytochrome P450 2E1, and alcohol produce combined mitochondrial injury and cytotoxicity in hepatoma cells. *Gastroenterology* 2005; **128**: 96–107.
8. Moriya K, Nakagawa K, Santa T, *et al.* Oxidative stress in the absence of inflammation in a mouse model for hepatitis C virus-associated hepatocarcinogenesis. *Cancer Res* 2001; **61**: 4365–70.
9. Korenaga M, Wang T, Li Y, *et al.* Hepatitis C virus core protein inhibits mitochondrial electron transport and increases reactive oxygen species (ROS) production. *J Biol Chem* 2005; **280**: 37481–8.
10. Lohmann V, Korner F, Koch J, Herian U, Theilmann L, Bartenschlager R. Replication of subgenomic hepatitis C virus RNAs in a hepatoma cell line. *Science* 1999; **285**: 110–3.
11. Ikeda M, Abe K, Dansako H, Nakamura T, Naka K, Kato N. Efficient replication of a full-length hepatitis C virus genome, strain O, in cell culture, and development of a luciferase reporter system. *Biochem Biophys Res Commun* 2005; **329**: 1350–9.
12. Ikeda M, Abe K, Yamada M, Dansako H, Naka K, Kato N. Different anti-HCV profiles of statins and their potential for combination therapy with interferon. *Hepatology* 2006; **44**: 117–25.

13. Setsukinai K, Urano Y, Kakinuma K, Majima HJ, Nagano T. Development of novel fluorescence probes that can reliably detect reactive oxygen species and distinguish specific species. *J Biol Chem* 2003; **278**: 3170–5.
14. Susin SA, Larochette N, Geuskens M, Kroemer G. Purification of mitochondria for apoptosis assays. *Methods Enzymol* 2000; **322**: 205–8.
15. Jarreta D, Orus J, Barrientos A, *et al.* Mitochondrial function in heart muscle from patients with idiopathic dilated cardiomyopathy. *Cardiovasc Res* 2000; **45**: 860–5.
16. Yamamoto A, Hoshi K, Ichihara K. Fluvastatin, an inhibitor of 3-hydroxy-3-methylglutaryl-CoA reductase, scavenges free radicals and inhibits lipid peroxidation in rat liver microsomes. *Eur J Pharmacol* 1998; **361**: 143–9.
17. Jones SP, Teshima Y, Akao M, Marban E. Simvastatin attenuates oxidant-induced mitochondrial dysfunction in cardiac myocytes. *Circ Res* 2003; **93**: 697–9.
18. Cadenas E, Boveris A, Ragan CI, Stoppani AO. Production of superoxide radicals and hydrogen peroxide by NADH-ubiquinone reductase and ubiquinol-cytochrome *c* reductase from beef-heart mitochondria. *Arch Biochem Biophys* 1977; **180**: 248–57.
19. Turrens JF, Boveris A. Generation of superoxide anion by the NADH dehydrogenase of bovine heart mitochondria. *Biochem J* 1980; **191**: 421–7.
20. Turrens JF, Alexandre A, Lehninger AL. Ubisemiquinone is the electron donor for superoxide formation by complex III of heart mitochondria. *Arch Biochem Biophys* 1985; **237**: 408–14.
21. Higuchi M, Proske RJ, Yeh ET. Inhibition of mitochondrial respiratory chain complex I by TNF results in cytochrome *c* release, membrane permeability transition, and apoptosis. *Oncogene* 1998; **17**: 2515–24.
22. Imai Y, Kawata S, Tamura S, *et al.* Relation of interferon therapy and hepatocellular carcinoma in patients with chronic hepatitis C. Osaka Hepatocellular Carcinoma Prevention Study Group. *Ann Intern Med* 1998; **129**: 94–9.
23. Shiratori Y, Imazeki F, Moriyama M, *et al.* Histologic improvement of fibrosis in patients with hepatitis C who have sustained response to interferon therapy. *Ann Intern Med* 2000; **132**: 517–24.
24. Jain SK, Pemberton PW, Smith A, *et al.* Oxidative stress in chronic hepatitis C: not just a feature of late stage disease. *J Hepatol* 2002; **36**: 805–11.
25. Furutani T, Hino K, Okuda M, *et al.* Hepatic iron overload induces hepatocellular carcinoma in transgenic mice expressing the hepatitis C virus polyprotein. *Gastroenterology* 2006; **130**: 2087–98.
26. Hino K, Kitase A, Satoh Y, *et al.* Interferon retreatment reduces or delays the incidence of hepatocellular carcinoma in patients with chronic hepatitis C. *J Viral Hepat* 2002; **9**: 370–6.
27. Hino K, Okita K. Interferon therapy as chemoprevention of hepatocarcinogenesis in patients with chronic hepatitis C. *J Antimicrob Chemother* 2004; **53**: 19–22.
28. Fartoux L, Degos F, Trepo C, *et al.* Effect of prolonged interferon therapy on the outcome of hepatitis C virus-related cirrhosis: a randomized trial. *Clin Gastroenterol Hepatol* 2007; **5**: 502–7.
29. O'Leary JG, Chan JL, McMahon CM, Chung RT. Atorvastatin does not exhibit antiviral activity against HCV at conventional doses: a pilot clinical trial. *Hepatology* 2007; **45**: 895–8.

Liver International (2008)

Journal of General Virology (2008), **89**, 1231–1242 DOI 10.1099/vir.0.83510-0

Hepatitis C virus NS5A protein interacts with and negatively regulates the non-receptor protein tyrosine kinase Syk

Sachiko Inubushi,[1]† Motoko Nagano-Fujii,[1]† Kikumi Kitayama,[1] Motofumi Tanaka,[1] Chunying An,[1] Hiroshi Yokozaki,[2] Hirohei Yamamura,[3] Hideko Nuriya,[4] Michinori Kohara,[4] Kiyonao Sada[1]‡ and Hak Hotta[1]

Correspondence
Hak Hotta
hotta@kobe-u.ac.jp

[1]Division of Microbiology, Kobe University Graduate School of Medicine, Kobe 650-0017, Japan

[2]Division of Surgical Pathology, Kobe University Graduate School of Medicine, Kobe 650-0017, Japan

[3]Hyogo Laboratory, Hyogo Prefectural Institute of Public Health and Environmental Sciences, Kobe 652-0032, Japan

[4]Department of Microbiology and Cell Biology, The Tokyo Metropolitan Institute of Medical Science, Tokyo 113-8613, Japan

Hepatitis C virus (HCV) is the major causative agent of hepatocellular carcinoma. However, the precise mechanism underlying the carcinogenesis is yet to be elucidated. It has recently been reported that Syk, a non-receptor protein tyrosine kinase, functions as a potent tumour suppressor in human breast carcinoma. This study first examined the possible effect of HCV infection on expression of Syk *in vivo*. Immunohistochemical analysis revealed that endogenous Syk, which otherwise was expressed diffusely in the cytoplasm of normal hepatocytes, was localized near the cell membrane with a patchy pattern in HCV-infected hepatocytes. The possible interaction between HCV proteins and Syk in human hepatoma-derived Huh-7 cells was then examined. Immunoprecipitation analysis revealed that NS5A interacted strongly with Syk. Deletion-mutation analysis revealed that an N-terminal portion of NS5A (aa 1–175) was involved in the physical interaction with Syk. An *in vitro* kinase assay demonstrated that NS5A inhibited the enzymic activity of Syk and that, in addition to the N-terminal 175 residues, a central portion of NS5A (aa 237–302) was required for inhibition of Syk. Moreover, Syk-mediated phosphorylation of phospholipase C-γ1 was downregulated by NS5A. An interaction of NS5A with Syk was also detected in Huh-7.5 cells harbouring an HCV RNA replicon or infected with HCV. In conclusion, these results demonstrated that NS5A interacts with Syk resulting in negative regulation of its kinase activity. The results indicate that NS5A may be involved in the carcinogenesis of hepatocytes through the suppression of Syk kinase activities.

Received 11 October 2007
Accepted 14 January 2008

INTRODUCTION

Hepatitis C virus (HCV) is the major aetiological agent of viral hepatitis worldwide after hepatitis A and B viruses (Choo *et al.*, 1989), with about 170 million people being infected. The majority of HCV-infected individuals develop chronic infection, which may progress to liver cirrhosis and hepatocellular carcinoma (HCC). HCV is a member of the family *Flaviviridae* and its genome consists of a single-stranded, positive-sense RNA of approximately 9600 nt, which encodes a polyprotein precursor of about 3010 aa. Currently, clinical HCV isolates are classified into six genotypes and more than 60 subtypes (Doi *et al.*, 1996; Mellor *et al.*, 1995; Robertson *et al.*, 1998). The polyprotein is cleaved by signal peptidase, signal peptide peptidase and two virally encoded proteases to generate at least ten mature proteins: core, envelope glycoprotein 1 (E1), E2, p7, non-structural protein 2 (NS2), NS3, NS4A, NS4B, NS5A and NS5B (Okamoto *et al.*, 2004; Reed & Rice, 2000).

HCV NS5A is part of the replication complex that catalyses replication of the viral genome. NS5A takes two forms, p56 and p58, with different degrees of phosphorylation, which may play distinct roles in the virus replication cycle (Evans

†These authors contributed equally to this work.

‡Present address: Division of Microbiology, Department of Pathological Sciences, Faculty of Medical Sciences, University of Fukui, Fukui 910-1193, Japan.

et al., 2004; Song *et al.*, 1999). The SNARE-like membrane fusion proteins VAP-A and VAP-B have been reported to interact with NS5A, and the binding capacity is inversely correlated to the degree of NS5A phosphorylation (Evans *et al.*, 2004; Gao *et al.*, 2004; Hamamoto *et al.*, 2005). NS5A binds to and inhibits double-stranded RNA-dependent protein kinase (PKR) (Gale *et al.*, 1998) and 2′,5′-oligoadenylate synthetase (Taguchi *et al.*, 2004). NS5A seems to have the potential to regulate not only interferon responses but also many other cellular functions, such as mitogenic signalling, apoptosis, the cell cycle and reactive oxygen species signalling, by interacting with a variety of host proteins (Macdonald *et al.*, 2004). These NS5A-interacting proteins include SRCAP (Ghosh *et al.*, 2000), Grb2 (He *et al.*, 2002; Tan *et al.*,1999), p53 (Majumder *et al.*, 2001; Qadri *et al.*, 2002), phosphatidylinositol 3-kinase p85 subunit (He *et al.*, 2002; Street *et al.*, 2004), karyopherin $\beta 3$ (Chung *et al.*, 2000), apolipoprotein A1 (Shi *et al.*, 2002), amphiphysin II (Zech *et al.*, 2003) and Src family protein tyrosine kinases (Macdonald & Harris, 2004; Macdonald *et al.*, 2004).

The non-receptor protein tyrosine kinase Syk is widely expressed in cells of the haematopoietic lineage, endothelium, epithelium and hepatocytes (Coopman *et al.*, 2000; Sada *et al.*, 2001; Tsuchida *et al.*, 2000; Turner *et al.*, 2000; Yanagi *et al.*, 1995, 2001). Syk contains tandem SH2 and kinase domains that are connected by an inter-SH2 domain and a linker region (Taniguchi *et al.*, 1991). The tandem SH2 domains of Syk bind to diphosphorylated immunoreceptor tyrosine-based activation motifs [ITAMs: $YXX(L/I)X_{6-8}YXX(L/I)$] in the cytoplasmic tail of the Fc receptor γ-chain or B-cell receptor subunit Igα to be activated after the engagement of immune receptors (Kurosaki *et al.*, 1995; Sada *et al.*, 2001; Shiue *et al.*, 1995; Turner *et al.*, 1995; Weiss & Littman, 1994). Autophosphorylation of Syk on Tyr^{525} and Tyr^{526} in the activation loop of the kinase domain results in an increase in its intrinsic kinase activity to phosphorylate its downstream signalling molecules, such as phospholipase C (PLC)-γ (Kurosaki *et al.*, 1995). Autophosphorylation on Tyr^{352} in the linker region is required for tyrosine phosphorylation of PLC-γ1 (Law *et al.*, 1996). Genetic studies have demonstrated that Syk is required for the development and maturation of B cells, mast-cell activation and platelet aggregation (Cheng *et al.*, 1995; Costello *et al.*, 1996; Poole *et al.*, 1997; Turner *et al.*, 1995, 2000). Furthermore, it has been reported that Syk functions as a tumour suppressor in breast cancers and that loss of Syk expression appears to be associated with malignant phenotypes (Coopman *et al.*, 2000).

In the present study, we demonstrated that HCV NS5A interacts physically with Syk to inhibit its kinase activity in human hepatoma-derived Huh-7 cells. Our results indicate that NS5A-induced downregulation of the possible tumour suppressor Syk may play a role in malignant transformation of HCV-infected hepatocytes.

METHODS

Expression plasmids. Mammalian expression plasmids for each of the Myc-tagged HCV proteins were constructed by amplifying and subcloning the corresponding cDNA fragments of pFK5B/2884Gly (Lohmann *et al.*, 2001) in frame to the pEF1/Myc-His(−) vector (Invitrogen). pFK5B/2884Gly was a kind gift from Dr R. Bartenschlager (University of Heidelberg, Germany). An expression plasmid for a polyprotein consisting of NS3–NS5B was amplified from pFK5B/2884Gly and subcloned into pEF1/Myc-His(−). Deletion mutants of NS5A were also amplified by PCR and subcloned into pEF1/Myc-His(−). Point mutations in NS5A [Tyr^{118} to Phe (Y118F), Val^{121} to Ala (V121A)] were introduced into pEF1/NS5A-Myc-His(−) by site-directed mutagenesis. Human Syk cDNA was a gift from Dr B. Müller-Hilke (University of Rostock, Germany). cDNA fragments for FLAG-tagged truncated forms and the kinase-inactive form of Syk were generated by PCR. All mutant forms of FLAG-tagged Syk were subcloned into pcDNA3.1/Hygro(+) (Invitrogen).

Cells, HCV RNA replicon and virus. Huh-7 human hepatoma-derived cells were maintained in Dulbecco's modified Eagle's medium supplemented with 10 % heat-inactivated fetal calf serum (FCS). Huh-7.5 cells (Blight *et al.*, 2002) were kindly provided by Dr C. M. Rice (The Rockefeller University, USA). BJAB cells, a human B-cell line expressing endogenous Syk, were cultured in RPMI 1640 supplemented with 10 % FCS.

Huh-7.5 cells stably harbouring an HCV subgenomic RNA replicon were prepared by using pFK5B/2884Gly, as described previously (Hidajat *et al.*, 2005; Lohmann *et al.*, 2001; Taguchi *et al.*, 2004; Takigawa *et al.*, 2004).

The plasmid pFL-J6/JFH1 encoding the entire genome of the HCV J6/JFH-1 strain was kindly provided by Dr C. M. Rice, and cell-free virus was propagated in Huh-7.5 cell cultures, as described previously (Lindenbach *et al.*, 2005).

Protein expression. Protein expression was performed using a recombinant vaccinia virus expressing T7 RNA polymerase (vTF7-3), as described previously (Deng *et al.*, 2006; Muramatsu *et al.*, 1997). In some experiments, protein expression was performed using a plasmid-based expression system without vTF7-3. For BJAB cells, we used an electroporation method (Schneider & Kieser, 2004). In brief, 3×10^6 cells were washed once with PBS and incubated for 10 min with 15 μg plasmid DNA in 250 μl RPMI 1640. Electroporation was carried out in a 4 mm cuvette using a Bio-Rad Gene Pulser II with a capacity of 975 μF and a voltage of 180 V. Immediately after electroporation, 500 μl FCS was added to the cells, which were then transferred to 4.5 ml RPMI 1640.

To activate Syk under hyperosmolarity conditions, cells were incubated with serum-free medium containing 400 mM sorbitol for 30 min at 37 °C, as described previously (Miah *et al.*, 2004). In addition, cells were treated with sodium pervanadate (generated by mixing 0.1 mM Na_3VO_4 with 1 mM H_2O_2) for 30 min to activate Syk (Wienands *et al.*, 1996).

Immunohistochemistry. Human normal adult liver autopsy materials and surgically resected liver tissue of patients with HCV-associated HCC were obtained with written informed consent. The tissues were fixed with 10 % buffered formalin, embedded in paraffin and sectioned. Immunohistochemical staining was performed with a Dako EnVision+ kit, according to the manufacturer's instructions. In brief, fixed sections were depleted of paraffin by treatment with xylene, dehydrated in ethanol and incubated with 3 % H_2O_2 to quench endogenous peroxidase activity. After being autoclaved at 121 °C for 20 min, the sections were incubated with a blocking

solution and then with anti-Syk rabbit polyclonal antibody (N-19; Santa Cruz Biotech). Normal rabbit IgG served as a control. The sections were then incubated with horseradish peroxidase-labelled polymer-conjugated secondary antibody. The sections were counter-stained with haematoxylin and examined under a light microscope. To confirm the specificity of immunostaining, anti-Syk antibody was pre-incubated with a 1000-fold excess of blocking peptide (Santa Cruz Biotech) for 2 h at room temperature prior to staining.

Detection of HCV RNA by *in situ* RT-PCR. *In situ* RT-PCR was performed as described previously (Maeda *et al.*, 2004) with some modifications. Briefly, OCT-embedded frozen liver biopsy sections were fixed with 10 % formaldehyde and treated with proteinase K. The samples were subjected to *in situ* reverse transcription using Moloney murine leukemia virus reverse transcriptase with an antisense primer for HCV (nt 290–272; 5′-AGTACCACAA GGCCTTTCG-3′), followed by *in situ* PCR using an *in situ* PCR System 1000 (Applied Biosystems) in the reaction mixture containing the antisense and a sense primer (nt 129–147; 5′-CCGGGAGAG CCATAGTGGT-3′). After being fixed in 4 % paraformaldehyde, the PCR products were detected by *in situ* hybridization using a digoxigenin (DIG)-labelled oligonucleotide probe, 5′-(DIG)-ATTTGGGCTGTGCCCCCGCGAGACTGCTAGCCGAGTAGTGTT-GGGT-$(DIG)_n$-3′ (nt 225–270). Anti-DIG antibody conjugated with alkaline phosphatase (Roche) was used to detect the probe. The slides were incubated in a dye solution containing nitro blue tetrazolium, 5-bromo-4-chloro-3-indolylphosphate and levamizole to yield a purplish-blue precipitate.

Immunoprecipitation and Western blotting. Cultured cells were lysed with a buffer containing 1 % Triton X-100, 50 mM Tris/HCl (pH 7.4), 150 mM NaCl, 10 mM EDTA, 1 mM NaF, 1 mM Na_3VO_4 and 1 mM PMSF. The lysate was centrifuged at 12 000 ***g*** for 20 min at 4 °C and the supernatant was immunoprecipitated with appropriate antibodies. In the case of liver tissue, each tissue sample was placed in a tube containing glass beads (1 mm diameter; BioSpec Products) to which 1 ml lysis buffer was added. The tube was then shaken at 4 °C for 3 min using a Mini-BeadBeater (BioSpec Products) to homogenize the tissues. After centrifugation at 80 ***g*** for 3 min, the supernatant was collected for immunoprecipitation analysis.

Immunoprecipitation and Western blot analyses were performed as described previously (Deng *et al.*, 2006). In brief, the supernatants of the lysates were pre-cleared with control IgG and protein A–Sepharose 4 Fast Flow (GE Healthcare) and incubated with appropriate antibodies at 4 °C for 1 h, followed by incubation with protein A–Sepharose 4 Fast Flow for another 1 h. After six washes with lysis buffer, the immunoprecipitates were analysed by Western blotting.

Antibodies used were as follows: anti-FLAG rabbit polyclonal antibody (Sigma); anti-Myc polyclonal and monoclonal antibodies (Santa Cruz Biotech); anti-Syk monoclonal antibody (4D10; Santa Cruz Biotech); anti-phospho Syk(Tyr^{352}) and Syk($Tyr^{525/526}$) rabbit polyclonal antibodies (Cell Signaling Technology); anti-PLC-γ1 monoclonal antibody (BD Biosciences); mouse monoclonal antibodies against core (Yasui *et al.*, 1998), NS3, NS4A and NS5A (kind gifts from Dr I. Fuke, Osaka University, Japan); anti-NS5A rabbit polyclonal antibody (NS5ACL1; a kind gift from Dr K. Shimotohno, Kyoto University, Japan; Miyanari *et al.*, 2007); and anti-NS5B goat polyclonal antibody (sc-17532; Santa Cruz Biotech). Normal IgG served as a control.

***In vitro* protein kinase assay.** An *in vitro* protein kinase assay was performed as reported previously (Miah *et al.*, 2004; Sada *et al.*, 2000, 2001). In brief, immunoprecipitates obtained with anti-Syk antibody from differentially transfected cells were incubated with 10 μg H2B histone (Sigma) as substrate in 20 μl kinase buffer, composed of 30 mM HEPES (pH 7.5), 10 mM $MgCl_2$, 2 mM $MnCl_2$, 4 μM ATP and 4 μCi (148 kBq) [γ-^{32}P]ATP, for 30 min at room temperature. Reactions were terminated by boiling for 5 min in 2 × sample buffer.

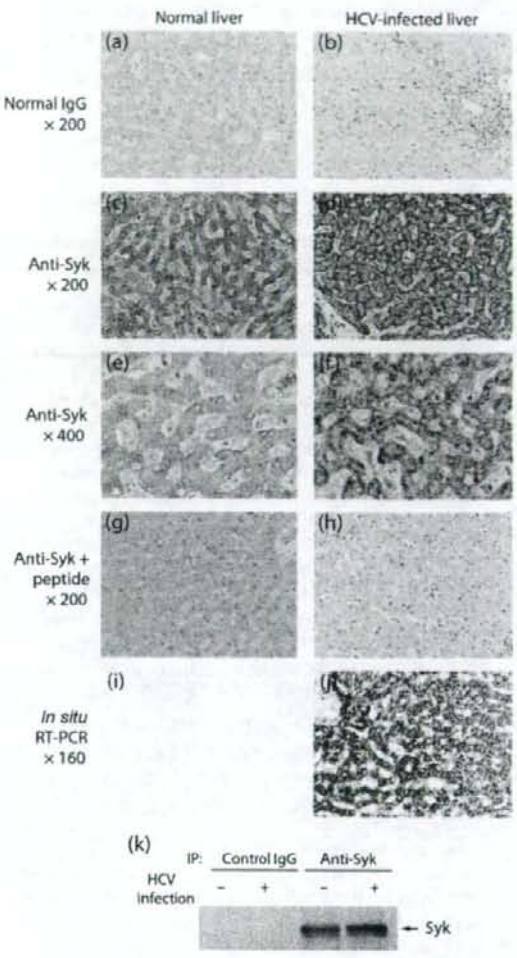

Fig. 1. Endogenous Syk expression in human liver tissues *in vivo*. Normal liver tissues (a, c, e, g, i) and HCV-infected non-cancerous liver tissues (b, d, f, h, j) were analysed. Formalin-fixed samples were stained with control IgG (a, b) or anti-Syk polyclonal antibody without (c–f) or with (g, h) pre-incubation with an excess amount of the immunogenic peptides. Frozen tissues were sectioned and examined for the presence of HCV RNA by *in situ* RT-PCR (i, j). Representative results are shown from four normal livers and ten HCV-infected livers. (k) Western blot analysis of normal human liver and HCV-infected non-cancerous liver. Supernatants of liver tissue homogenates (1.75 mg protein equivalent) were immunoprecipitated with anti-Syk monoclonal antibody (4D10) and probed with the same antibody or with control IgG.

Proteins were separated by SDS-PAGE. The gels were treated with 1 M KOH for 1 h at 56 °C to remove phosphoserine and most of the phosphothreonine. After gel drying, radiolabelled proteins were visualized by autoradiography. For quantitative analysis, γ-^{32}P incorporation was measured using a PhosphorImager (BAS2000; Fuji) and protein amounts with an LAS1000 image analyser (Fuji).

RESULTS

Different expression patterns of endogenous Syk in normal and HCV-infected liver tissues

We first examined whether Syk was expressed in human liver tissues. Immunohistochemical analysis revealed that Syk was indeed expressed and rather diffusely distributed throughout the cytoplasm of normal adult hepatocytes (Fig. 1c, e). This pattern was observed with four out of four normal liver tissues (100 %; data not shown). The specificity of the staining was verified by pre-incubating the antibody with an excess amount of the immunogenic peptides (Fig. 1g, h). We then examined Syk expression in non-cancerous liver tissue obtained from patients with HCV-associated HCC. Interestingly, Syk was detected near the plasma membrane with a patchy pattern in hepatocytes of eight out of ten HCV-infected patients (80 %; Fig. 1d, f, and data not shown). All of the specimens stained with normal rabbit IgG were negative (Fig. 1a, b). We confirmed that almost all of the hepatocytes in the tissue samples were infected with HCV using *in situ* RT-PCR (Fig. 1i, j).

Western blot analysis confirmed Syk expression in human liver tissue, irrespective of HCV infection (Fig. 1k). It should be noted, however, that the Syk expression was rather weak, as we could achieve successful Western blotting only after the tissue lysates were concentrated by immunoprecipitation with specific antibody. Also, possibly due to the low level of expression and comparatively low sensitivity of the antibodies used for Western blotting, we could not detect the phosphorylated forms of Syk in the liver tissue (data not shown).

Identification of Syk as a novel NS5A-interacting protein

We then examined the possible interaction between HCV proteins and Syk in cultured cells. For this purpose, various HCV proteins and Syk were expressed ectopically in Huh-7 cells, as these cells do not express endogenous Syk. Co-immunoprecipitation analysis revealed that NS5A associated with Syk, whereas the other HCV proteins associated with Syk very weakly or not at all (Fig. 2a, b). A specific interaction of NS5A with Syk was also observed when NS5A was expressed as part of an NS3–NS5B polyprotein (Fig. 2c). These results collectively suggested that NS5A interacts specifically with Syk.

Next, we examined the possible interaction of NS5A with endogenously expressed Syk. As human hepatoma-derived cell lines, such as Huh-7, HepG2 and FLC4, are negative for

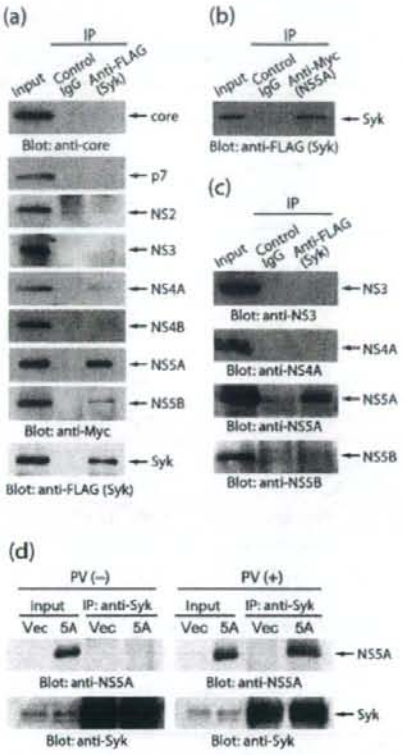

Fig. 2. NS5A specifically interacts with Syk in Huh-7 cells. (a) Each of the Myc-tagged HCV proteins was expressed with FLAG-tagged full-length Syk. Cell lysates were immunoprecipitated using anti-FLAG antibody or control IgG. Cell lysates (input) and the immunoprecipitates were probed with anti-core or anti-Myc antibodies. A representative result verifying efficient immunoprecipitation is shown at the bottom. (b) Myc-tagged NS5A was expressed with FLAG-tagged full-length Syk. Cell lysates were immunoprecipitated using anti-Myc antibody or control IgG, and probed with anti-FLAG antibody. (c) A polyprotein consisting of NS3–NS5B was expressed with FLAG-tagged Syk. Cell lysates were immunoprecipitated with anti-FLAG antibody or control IgG, and probed with the indicated antibodies. (d) NS5A was expressed in BJAB cells expressing endogenous Syk. The cells were treated with pervanadate (PV) or left untreated. Cell lysates were immunoprecipitated with anti-Syk monoclonal antibody and probed with anti-NS5A or anti-Syk monoclonal antibody. Vec, control using empty vector.

endogenous Syk expression, we used BJAB cells endogenously expressing Syk. Unlike ectopically expressed Syk, endogenous Syk in BJAB cells is not tyrosine phosphorylated. Therefore, we treated the cells with pervanadate to induce tyrosine phosphorylation of Syk. Co-immunoprecipitation experiments clearly demonstrated that NS5A

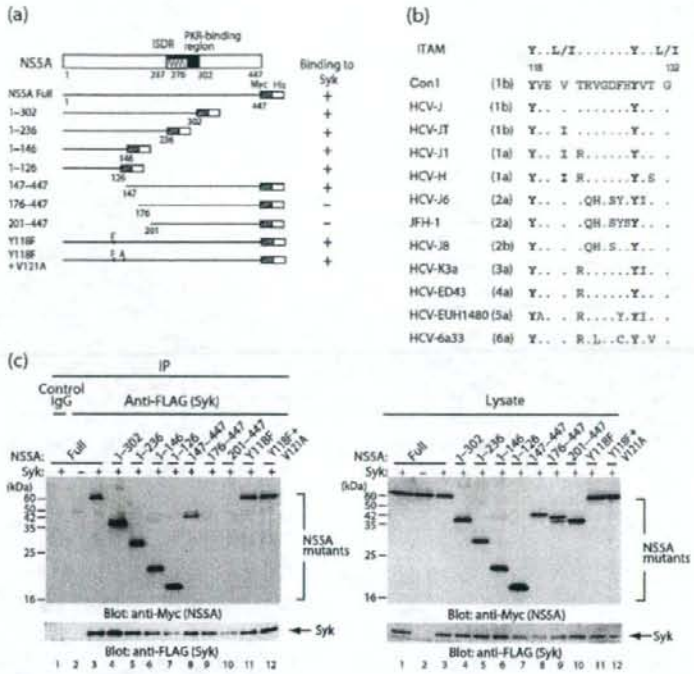

Fig. 3. Determination of the Syk-binding region(s) of NS5A. (a) Schematic diagram of various deletion mutants of NS5A and their Syk-binding capacity. (b) Alignment of amino acid sequences surrounding the ITAM-related sequence in NS5A of various HCV strains. The genotype is indicated in parentheses. Residues identical to those of HCV strain Con1 are shown by a dot. Residues identical to ITAM are shown in bold. (c) Full-length (Full) and a series of deletion mutants of Myc-tagged NS5A were expressed in Huh-7 cells with or without FLAG-tagged full-length Syk. Cell lysates were immunoprecipitated using anti-FLAG antibody and probed with anti-Myc antibody (left panel). Efficient immunoprecipitation was verified (bottom). Cell lysates were probed directly with anti-Myc and anti-FLAG antibodies to verify comparable expression levels of the NS5A mutants and Syk, respectively (right panels).

interacted with endogenous Syk when the cells were treated with pervanadate, but not when the cells were left untreated (Fig. 2d).

The N-terminal region of NS5A is required for interaction with Syk

To map a Syk-interacting region(s) of NS5A, interaction between various deletion mutants of NS5A and Syk was tested. C-terminally deleted mutants of NS5A up to aa 126, as well as the full-length NS5A, were co-immunoprecipitated with Syk (Fig. 3a, c). This result suggested that neither the PKR-binding region nor the interferon sensitivity-determining region (ISDR) of NS5A was required for the interaction with Syk. A proline-rich region of NS5A (aa 343–356), which is reported to bind to the Src family kinases (Macdonald & Harris, 2004; Macdonald *et al.*, 2004), was not involved in the Syk interaction either. In contrast, the N-terminally truncated mutant of NS5A(147–447), but not the further truncated mutants NS5A(176–447) or NS5A(201–447), was co-immunoprecipitated with Syk, suggesting that a region of NS5A between aa 147 and 175 is also involved in the interaction with Syk. We also observed that NS5A(1–126) and NS5A(174–447), but not NS5A(201–447), interacted with Syk(1–261) or Syk(379–635) (data not shown). These results collectively suggested that NS5A interacts with Syk through two independent regions of NS5A (aa 1–126 and 147–175).

Syk is activated by interaction with a diphosphorylated ITAM of immune receptors (Sada *et al.*, 2001; Turner *et al.*, 2000; Weiss & Littman, 1994). NS5A from HCV strain Con1 possesses a sequence (AEEY^{118}VEV^{121}-TRVGDFHY^{129}VTG) that resembles an ITAM (Fig. 3b). We found that the two tyrosine residues at positions 118 and 129 are highly conserved across different genotypes and subtypes. The tyrosine at position 118 is exposed on

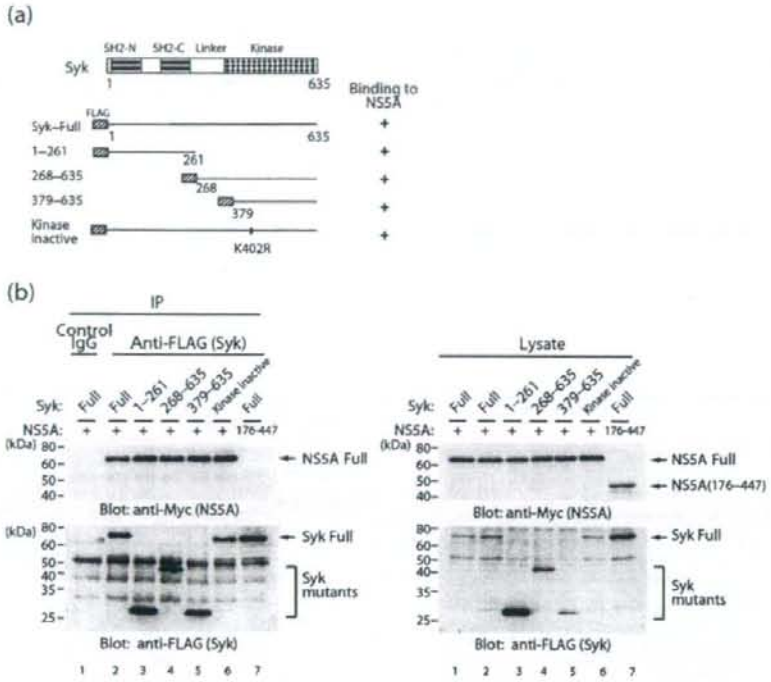

Fig. 4. NS5A interacts with both N-terminal and C-terminal regions of Syk. (a) Schematic diagram of the deletion mutants of Syk and their NS5A-binding capacity. (b) Full-length (Full) and a series of domain-deletion mutants of FLAG-tagged Syk was expressed in Huh-7 cells with Myc-tagged full-length NS5A (lanes 1–6) or NS5A(176–447) (lane 7). Cell lysates were immunoprecipitated using anti-FLAG antibody and probed with anti-Myc antibody (left upper panel). Efficient immunoprecipitation of Syk deletion mutants was verified (bottom). Cell lysates were probed directly with anti-Myc and anti-FLAG antibodies to verify comparable expression levels of the NS5A and Syk mutants, respectively (right panels).

the surface of the NS5A molecule (Tellinghuisen *et al.*, 2005). We examined whether this sequence motif was involved in the interaction with Syk. A single point mutation of Tyr^{118} (Y118F) or double mutations of Tyr^{118} and Val^{121} (Y118F and V121A) in NS5A did not affect the interaction with Syk (Fig. 3c, lanes 11 and 12). Thus, it is unlikely that NS5A binds to Syk through its ITAM-related sequence in the same manner as that observed for immune receptors.

To map the NS5A-binding region in Syk, a series of domain-deleted mutants of Syk was examined. The results obtained revealed that both N-terminal (tandem SH2 domains) and C-terminal halves (linker and the kinase domain) interacted with NS5A (Fig. 4). The kinase domain alone and a kinase-inactive form of Syk were also co-immunoprecipitated with NS5A. These results suggested that the NS5A–Syk interaction occurs through the N- and C-terminal regions of Syk and that the catalytic activity of Syk is not necessary for the interaction.

NS5A expression downregulates the kinase activity of Syk

Next, we tested the possible effect of NS5A expression on Syk kinase activity. An *in vitro* kinase assay revealed that full-length NS5A and a C-terminally deleted NS5A(1–302) mutant significantly inhibited Syk kinase activity (Fig. 5, lanes 2–4). In contrast, NS5A(1–236), which lacked both the PKR-binding region (aa 237–302) and ISDR (aa 237–276), failed to inhibit Syk kinase activity, although it could interact with Syk. NS5A(176–447), which contained the PKR-binding region and ISDR but lacked the Syk-binding region, did not affect Syk kinase activity. These results collectively suggested that NS5A requires both N-terminal (aa 1–175) and central (aa 237–302) regions for the downregulation of Syk kinase activity (Table 1).

To address the relevance of the interaction between NS5A and Syk, the possible effect(s) of NS5A on Syk-mediated cellular signalling in Huh-7 cells was examined. Ectopic

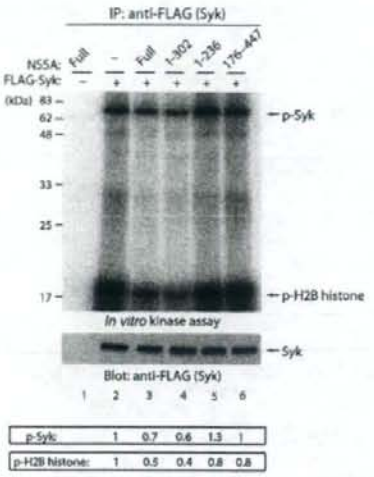

Fig. 5. NS5A downregulates Syk kinase activity. Myc-tagged NS5A and FLAG-tagged Syk were expressed in Huh-7 cells. Cell lysates were immunoprecipitated with anti-FLAG antibody and the immunoprecipitates were subjected to an *in vitro* kinase assay using H2B histone as substrate. Phosphorylation of Syk (p-Syk) and H2B histone (p-H2B histone) was visualized by autoradiography (upper panel). Efficient immunoprecipitation of Syk was verified (lower panel). Arbitrary units of Syk kinase activities, represented by the phosphorylation values of p-Syk and p-H2B histone normalized to the amounts of immunoprecipitated Syk, are shown at the bottom.

expression of Syk alone mediated signal transduction to induce tyrosine phosphorylation of a wide variety of cellular proteins, either directly or indirectly (Fig. 6a, lanes 1 and 3). Hyperosmolarity stress (400 mM sorbitol treatment) enhanced Syk-mediated tyrosine phosphorylation of cellular proteins (Fig. 6a, lanes 3 and 4), with the result being consistent with the previous observation (Miah *et al.*, 2004). Interestingly, co-expression of NS5A decreased Syk-mediated tyrosine phosphorylation of cellular proteins both in the absence and presence of hyperosmolarity stress (Fig. 6a, lanes 7 and 8). The phosphorylation of Syk on Tyr^{352} and/or $Tyr^{525/526}$ is a marker for Syk activation. Using these parameters, we confirmed that co-expression of NS5A inhibited Syk activation both in the absence and presence of hyperosmolarity stress (Fig. 6b).

PLC-γ1 has been reported to be a downstream molecule of Syk-mediated signal transduction (Law *et al.*, 1996). Our results demonstrated that NS5A inhibited PLC-γ1 phosphorylation, probably through downregulation of Syk kinase activity, both in the absence and presence of hyperosmolarity stress (Fig. 6c).

Table 1. Summary of NS5A deletion mutational analysis of the interaction with Syk and inhibition of Syk kinase activity

NS5A mutant	Interaction with Syk	Inhibition of Syk
NS5A(1–447; full)	+	+
NS5A(1–302)	+	+
NS5A(1–236)	+	–
NS5A(176–447)	–	–

NS5A expressed in the context of HCV RNA replication interacts with Syk in Huh-7.5 cells

The interaction of NS5A with Syk was examined further using Huh-7.5 cells harbouring an HCV subgenomic RNA replicon. The results obtained clearly demonstrated that NS5A expressed in the context of HCV RNA replication interacted with Syk (Fig. 7a). It is well known that NS5A takes two forms, p56 and p58, with the former being the basally phosphorylated form and the latter the hyperphosphorylated form (Kaneko *et al.*, 1994; Song *et al.*, 1999). It is noteworthy that Syk interacted with p56 more efficiently than with p58.

We also examined the interaction of NS5A with Syk in Huh-7.5 cells infected with the J6/JFH-1 strain of HCV. The results demonstrated that NS5A interacted with Syk in HCV-infected cells (Fig. 7b). These results collectively suggested that the NS5A–Syk interaction occurs in the context of virus replication, where NS5A is primarily utilized to form the viral replication complex. In this connection, HCV J6/JFH-1 replication was not affected significantly by ectopically expressed Syk in Huh-7.5 cells (data not shown). This observation, however, does not necessarily exclude the possibility that the NS5A interaction with Syk exerts certain biological effect(s) on the host cell's fate.

Syk kinase activity is suppressed in the context of HCV RNA replication

We then examined Syk kinase activity in the HCV subgenomic RNA-harbouring Huh-7.5 cells. An *in vitro* kinase assay demonstrated that Syk kinase activities, represented by autophosphorylation of Syk (p-Syk) and phosphorylation of a substrate (p-H2B histone), were significantly suppressed in HCV RNA-replicating cells compared with the control (Fig. 7c). These results suggested the possibility that Syk kinase activity is downregulated through an NS5A–Syk interaction in HCV-infected hepatocytes as well.

DISCUSSION

The non-receptor protein tyrosine kinase Syk is expressed in a wide variety of haematopoietic cell lineages (Taniguchi *et al.*, 1991). It is also expressed in human mammary